Journal of Engineering Physics and Thermophysics, Vol. 80, No. 3, 2007

FLUID AND GAS DYNAMICS IN TECHNOLOGICAL PROCESSES

STOCHASTIC MODELS OF PARTICLE MOTION IN A TURBULENT FLOW AND THEIR APPLICATION FOR CALCULATING INTERNAL FLOWS

K. N. Volkov

UDC 532.529:536.24

This paper considers issues connected with the construction and numerical realization of stochastic models of motion and scattering of condensed impurity particles in a turbulent flow based on the integration of a Langevin-type equation. The proposed model is used to calculate the turbulent flow of a low-concentration gas suspension in a channel with permeable walls. Calculations are performed for various values of the injection rate, sizes of particles, and the conditions of their introduction into the channel.

Introduction. To describe and forecast the properties of gas-disperse systems, the following approaches are used: kinetic, continual, and trajectory ones. Practical realization of a particular approach is dictated by the range of applicability and the possibility of forecasting various characteristics of the flow [1]. The kinetic approach finds application in constructing and justifying mathematical models of gas-dispersion media, in particular, for obtaining transfer equations of moments of fluctuating parameters of the gaseous and dispersed phases [2]. In solving specific problems, kinetic models are used comparatively seldom because of the difficulty of solving corresponding equations. In the continual approach, one considers the interpenetrative motion of several interacting continua connected with the gas and particles, which is described by the continuum mechanics equations in Euler variables. To close Reynolds-averaged equations, equations of the second moments of fluctuating parameters of the gaseous and dispersed phases are used. Correlation moments connected with the dispersed phase are found either on the basis of the probability density function method [2] or by the space-time averaging method [3]. In the trajectory approach, impurity motions are written in Lagrangian variables and integrated along the trajectories of individual particles in the known (precalculated) gas-dynamic field. Compared to the continual method, the trajectory approach requires simple and physically more correct closing assumptions, which makes it possible to elucidate the flow structure with a high degree of detailing. However, to simulate the impurity motion, a fairly representative ensemble of particles is needed [4].

Depending on whether or not the influence of velocity fluctuations of the carrier turbulent flow on the particle motion is taken into account, one distinguishes two variants of the trajectory approach [1, 4]: the deterministic and the stochastic ones. In the first variant, the interaction of a particle with turbulent moles is excluded from the consideration, which holds only for rather inertial particles. The position of the probe particle at the initial instant of time fully determines its further evolution. In the second variant, the decomposition of the velocity field of the carrier flow into a mean and a random component is used. The mean component is calculated on the basis of Reynolds-averaged Navier–Stokes equations closed by means of a particular turbulence model, direct numerical simulation, or modeling of large vortices. The random component is determined by the Monte Carlo method. In practice, various approaches to the numerical realization of the computational procedure for the random velocity component are used.

In the model of the turbulent mole lifetime, the turbulence field is modeled by a combination of spherical vortices, each of which is characterized by the velocity, size, and lifetime depending on the local characteristics of turbulence [1, 5]. The turbulent mole loses and acquires individuality stepwise, which leads to the appearance of fluctuations of the turbulent flow parameters. As a criterion of the random velocity component generation, the lowest value

D. F. Ustinov Baltic State Technical University "Voenmekh," 1 Krasnoarmeiskaya Str., St. Petersburg, 190005, Russia; email: dsci@mail.tu. Translated from Inzhenerno-Fizicheskii Zhurnal, Vol. 80, No. 3, pp. 136–147, May–June, 2007. Original article submitted September 12, 2005.

 1062-0125/07/8003-0570

of the vortex lifetime and the particle-vortex interaction time is usually chosen [5]. Comparison of different approaches shows that the realization of the stochastic model appears to be insensitive to the choice of the generation criterion of a new fluctuation of the carrier flow velocity [1]. The disadvantage of the model and its different modifications is that the pulsation fluid velocity field is not continuous, and the time dependence of the correlation coefficient is linear [1]. In a number of models, it is assumed that the time internal between sequential changes in the carrier flow velocity (vortex lifetime) is a random value distributed by the Poisson law [6].

The present paper considers another approach where the calculation of the fluctuation velocity component is based on the integration of a stochastic equation of the Langevin type [7]. The Langevin equation is used to describe either only the carrier flow [8, 9] or only the dispersed phase [10] or both of them [11]. The features of the formulation and realization of various stochastic models of impurity motion and scattering are given and their advantages and disadvantages are noted. The possibilities of the approach are demonstrated with the example of calculating the turbulent flow of a low-concentration gas suspension in a blow-distributed channel (the back influence of particles is ignored). Calculations are performed for various blow velocities and conditions of introduction of particles into the channel. Comparison of the results obtained on the basis of the deterministic and stochastic models is made.

Simulation of the Carrier Phase. The realization of the stochastic model requires calculations of both the medium and the pulsation velocity fields of the carrier flow. To this end, various approaches differing in the degree of detailing of the flow pattern and the difficulty of realization are used [1]. The approaches considered in [1] were used successfully to simulate flows of different classes, including the calculation of the impurity motion in an inhomogeneous turbulence field [12]. The current approaches to the turbulence simulation, such as simulation of large vortices or direct numerical simulation, permit weakening the dependence of calculation results on semiempirical data.

For simplicity, consider a one-dimensional case assuming $\langle u' \rangle = 0$ and considering the energy spectrum of turbulence and the correlation function to be given. They are related by the relation

$$R(x) = \langle u(x)\, u(x+r) \rangle = \int_{-\infty}^{+\infty} E(|\kappa|) \exp(2\pi i \kappa x)\, d\kappa .$$

To reproduce the velocity field of the carrier flow, one uses in the trajectory calculations of probe particles methods based on the statistical processing of data obtained as a result of solving filtered or complete Navier–Stokes equations. Such methods can be broken down into several groups.

1. The velocity is expressed as the Fourier integral

$$u(x) = \int_{0}^{+\infty} E^{1/2}(\kappa) \cos(2\pi\kappa x)\, dw_1(\kappa) + \int_{0}^{+\infty} E^{1/2}(\kappa) \sin(2\pi\kappa x)\, dw_2(\kappa) .$$

White noise is a random process with a zero mathematical expectation and a correlation function in the form of a delta function.

2. The velocity is given as the convolution

$$u(x) = \int_{-\infty}^{+\infty} G(x-r)\, dw(r) , \quad G(x) = \int_{-\infty}^{+\infty} E^{1/2}(|\kappa|) \cos(2\pi\kappa x)\, d\kappa .$$

3. To simulate a nonstationary velocity field, the wavelet (short wave packet) theory is used. The velocity is represented as the basis expansion

$$u(x) = \sum_{i,j=-\infty}^{+\infty} G_i(x)^{*}\, \varphi_{ij}(x)\, \xi_{ij} ,$$

where i, j = 0, ±1, ±2, and $\{\xi_{ij}\}_{-\infty}^{+\infty}$ is a sequence of independent random variables distributed by the normal law. The orthonormal basis is of the form

$$\varphi_{ij}(x) = 2^{i/2}\varphi(2^i x - j).$$

Substitution yields

$$u(x) = \sum_{i=-\infty}^{+\infty} u_i(2^i x), \quad u_i(x) = \sum_{j=-\infty}^{+\infty} f_i(x-j)\,\xi_{ij}.$$

Here

$$f_i(x) = G_i(x)^*\,\varphi(x); \quad G_i(x) = 2^{-i/2}\,G(2^{-i}x),$$

and $\varphi(x)$ is a Mayer wavelet.

Dispersed Phase Simulation. The equations describing the translational motion of a spherical probe particle are of the form

$$\frac{d\mathbf{r}_\mathrm{p}}{dt} = \mathbf{v}_\mathrm{p}, \tag{1}$$

$$\frac{d\mathbf{v}_\mathrm{p}}{dt} = \frac{3C_\mathrm{d}\rho}{8\rho_\mathrm{p} r_\mathrm{p}}\,|\mathbf{v}-\mathbf{v}_\mathrm{p}|\,(\mathbf{v}-\mathbf{v}_\mathrm{p}). \tag{2}$$

To calculate the resistance coefficient, the relation

$$C_\mathrm{d} = \frac{24}{\mathrm{Re}_\mathrm{p}} f_\mathrm{d}(\mathrm{Re}_\mathrm{p}).$$

is used. The function f_d takes into account the correction to the Stokes resistance law for the particle inertia. The Reynolds number for the motion of the particle and the carrier gas is found by the formula

$$\mathrm{Re}_\mathrm{p} = \frac{2r_\mathrm{p}\rho\,|\mathbf{v}-\mathbf{v}_\mathrm{p}|}{\mu}.$$

The dynamic relaxation time of the particle is calculated by the relation

$$\tau_\mathrm{p} = \frac{8}{3}\frac{\rho_\mathrm{p}}{\rho}\frac{r_\mathrm{p}}{C_\mathrm{d}\,|\mathbf{v}-\mathbf{v}_\mathrm{p}|}.$$

Equations (1) and (2) are integrated along the path of an individual particle and require specification of only the initial conditions — the coordinates and the particle velocity at the instant of time t = 0. The carrier gas velocity in Eq. (2) represents a random function of the spatial coordinates and time. The carrier flow turbulence is taken into account by introducing random velocity fluctuations into (2). The carrier gas velocity is given as a sum of the averaged component $\langle\mathbf{v}\rangle$ and the random variable $\mathbf{v}'$. The mean component is thought to be given (precalculated). To calculate the fluctuation component, a Langevin-type equation is used. Depending on the statement of the problem, different forms of writing the Langevin equation are used.

Inertialess Particle. To simulate the motion of an inertialess particle in a homogeneous isotropic turbulence field, the following stochastic equation is used [7]:

$$d\mathbf{v} = \mathbf{v}\,(t + dt) - \mathbf{v}\,(t) = -\frac{\mathbf{v}}{T_{\mathrm{L}}}\,dt + \sigma\left(\frac{2}{T_{\mathrm{L}}}\right)^{1/2} d\mathbf{w}\,. \tag{3}$$

Here $d\mathbf{w}$ is a Wiener random process (white noise), for which $\langle d\mathbf{w}\rangle = 0$, $\langle (d\mathbf{w})^2\rangle = dt$, $\langle dw_i(t) dw_j(t)\rangle = \delta_{ij} dt$. The velocity fluctuations are related to energy-containing vortices having a time scale T_{L}. The velocity dispersion is obtained from the relation

$$\left\langle (d\mathbf{v})^2 \right\rangle = \left\langle [\mathbf{v}\,(t + dt) - \mathbf{v}\,(t)]^2 \right\rangle = \frac{2\sigma^2}{T_{\mathrm{L}}}\,dt\,.$$

In the inertial, interval, the dispersion represents a linear function of time $\langle (d\mathbf{v})^2\rangle = C_{\mathrm{K}}\varepsilon dt$. Therefore, $T_{\mathrm{L}} = 4k/(3C_{\mathrm{K}}\varepsilon) = k/\varepsilon$, which serves as a physical basis of Eq. (3) used to simulate the diffusion of a fluid particle from a point source [9], the motion of inertialess particles in a turbulent flow [7, 10], and the passage to kinetic equations [13].

The multidimensional Markovian process, whose components satisfy the Langevin equation (3), can be compared to the Fokker–Planck equation for the probability density function. The solution of the latter shows that the mean-square Stokes particle displacement in the time interval dt is proportional to this interval:

$$\left\langle (d\mathbf{r})^2 \right\rangle = 2D dt\,.$$

To take into account the turbulence inhomogeneity, additional terms are added to Eq. (3) to provide a nonzero root-mean-square value of the random force (moments up to the sixth order are taken into account), and a mean pressure gradient is introduced [8]. However, third- and higher-order-moments play a secondary role compared to the second moments [14].

The model of [15] uses the assumption about the gradient character of the turbulent transfer, and the inertialess particle displacement is modelled on the basis of the equation

$$d\mathbf{r} = \frac{1}{\rho}\,\nabla\mu_{\mathrm{t}} dt + \left(\frac{2\mu_{\mathrm{t}}}{\rho}\right)^{1/2} d\mathbf{w}\,.$$

The turbulent viscosity is calculated by the Kolmogorov–Prandtl formula.

To take into account the correlation of velocities at different points of the space at various instants of time, Eq. (3) is given in a modified form. In the case of homogeneous turbulence, the velocity at time t^{n+1} is related to the velocity at time t^n by the relation [16, 17]

$$v_i^{n+1} = R_{ii}\,(t, x)\,v_i^n + \sigma_i\left[1 - R_{ii}^2\,(t, x)\right]^{1/2} \xi_i\,(t)\,. \tag{4}$$

In an inhomogeneous turbulence field, Eq. (4) is written in the following form [18]:

$$v_i^{n+1} = R_{ii}\,(t, x)\,v_i^n + \sigma_i\left[1 - R_{ii}^2\,(t, x)\right]^{1/2} \xi_i\,(t) + \left[1 - R_{ii}\,(t, x)\right] T_{\mathrm{L}ii}\,\frac{\partial\sigma_3}{\partial x_3}\,\delta_{i3}\,.$$

In the special case of the step correlation function used in [19], Eq. (4) takes the form

$$v_i^{n+1} = -\frac{\Delta t}{T_{\mathrm{L}ii}}\,v_i^n + \sigma_i\left[1 - \left(1 - \frac{\Delta t}{T_{\mathrm{L}ii}}\right)^2\right]^{1/2} \xi_i\,(t)\,.$$

The space-time correlation function is given as a product of the Lagrange and Euler correlations [20]:

$$R_{ii}\,(t, x) = R_{\mathrm{L}ii}\,(t)\,R_{\mathrm{E}ii}\,(x)\,.$$

In practice, various forms of the Lagrange correlation function are used [20], in particular, for $q > 0$

$$R_{\mathrm{L}ii}(t) = \exp\left[-\frac{t}{(q^2+1)\,T_{\mathrm{L}ii}}\right]\cos\left[\frac{qt}{(q^2+1)\,T_{\mathrm{L}ii}}\right],\ R_{\mathrm{L}ii}(t) = \exp\left(-\frac{t}{T_{\mathrm{L}ii}}\right).$$

The Euler correlation function is usually expressed in terms of the longitudinal $f(r)$ and transverse $g(r)$ correlation coefficients by means of the von Kármán relation [20]

$$R_{\mathrm{E}ii}(r) = [f(r) - g(r)]\,\frac{r_i r_j}{r^2} + g(r)\,\delta_{ij}\,.$$

These correlations coefficients for a homogeneous isotropic turbulence have the form

$$f(r) = \exp\left(-\frac{r}{L_{\mathrm{E}xx}}\right),\ \ g(r) = \left(1 - \frac{r}{2L_{\mathrm{E}yy}}\right)\exp\left(-\frac{r}{L_{\mathrm{E}yy}}\right).$$

The integral length scales are obtained from the relations $L_{\mathrm{E}xx} = 1.1T_{\mathrm{L}}\sigma$, $L_{\mathrm{E}yy} = L_{\mathrm{E}zz} = 0.5L_{\mathrm{E}xx}$.

Inertial Particle. In the model of [7], the pulsed motion of a particle is modeled on the basis of the stochastic equation

$$d\mathbf{v} = -\frac{\mathbf{v}_{\mathrm{p}}}{\tau_{\mathrm{p}}}\,dt + \sigma_{\mathrm{p}}\left(\frac{2}{\tau_{\mathrm{p}}}\right)^{1/2} d\mathbf{w}\,,$$

which coincides formally with (3) but is characterized by different time scales. In a homogeneous isotropic turbulence, the velocity dispersions of the particle and the carrier flow are related by the relation [20]

$$\frac{\sigma_{\mathrm{p}}^2}{\sigma^2} = \frac{1}{1 + \alpha\tau_{\mathrm{p}}/T_{\mathrm{L}}}\,,$$

where $\alpha \approx 1.0$. For a homogeneous isotropic turbulence, $\sigma^2 = 2k/3$ and $T_{\mathrm{L}} = \beta k/\varepsilon$, where $\beta = 0.11$–0.60. In the field of mass forces, the relative motion of the particle and the fluid element are taken into account [21].

In discrete form, the Lagrange equation is written as

$$\mathbf{v}^{n+1} = a\mathbf{v}^n + b\boldsymbol{\xi}^n\,, \tag{5}$$

where $\xi^n \cup N(0, 1)$. Multiplying relation (5) by $\mathbf{v}^n$, $\mathbf{v}^{n+1}$ and making averaging, we obtain

$$a = \frac{\langle \mathbf{v}^{n+1}\mathbf{v}^{n+1}\rangle}{\langle \mathbf{v}^n\mathbf{v}^n\rangle} = R_{\mathrm{L}}(t)\,,\ \ b^2 = \langle \mathbf{v}^{n+1}\mathbf{v}^{n+1}\rangle - a^2\,\langle \mathbf{v}^n\mathbf{v}^n\rangle = \sigma^2\left(1 - a^2\right).$$

Here $\sigma^2 = \langle \mathbf{v}^n\mathbf{v}^n\rangle$, $\xi^n(dt)^{1/2} \to d\mathbf{w}$ at $dt \to 0$, $dt = t^{n+1} - t^n$. When the exponential correlation function is used, the coefficients acquire the following values: $a = \exp(-\Delta t/T_{\mathrm{L}})$, $b = \sigma(1 - a^2)^{1/2}$. At $\tau_{\mathrm{p}} \to 0$ (light particles) the correlation function is Lagrangian, and at $\tau_{\mathrm{p}} \to \infty$ (heavy particles) it is Eulerian.

Variants of Lagrange Models. Consider a condensed particle P and a fluid particle F that coincide at some instant of time t^n (Fig. 1). Because of the inertia, their positions differ at the time t^{n+1}. To calculate the velocity of the fluid particle at the time t^{n+1}, either the one-step (Lagrange) or the two-step (Lagrange–Euler) approaches are used.

One-step approach. In the model of [22, 23], the fluid particle velocity at the instant of time t^{n+1} is expressed in terms of the velocity of this same particle at the instant of time t^n. The obtained value is used in the equations describing the motion of the condensed particle. The fluid particle velocity at the time t^{n+1} is given in the form

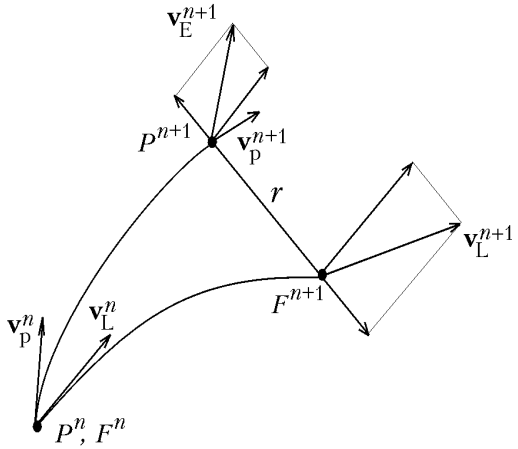

Fig. 1. To the calculation of the carrier turbulent flow velocity at the instant of time t^{n+1}.

$$\mathbf{v}_{\mathrm{L}}^{n+1} = a\mathbf{v}_{\mathrm{L}}^{n} + b\boldsymbol{\xi}^{n}.$$

The coefficients a and b are described by the same relations as for Eq. (5). Instead of the time scale T_{L}, the scale T_{L}^{*} is used. It is obtained with the aid of the linear interpolation

$$T_{\mathrm{L}}^{*} = \frac{\omega}{T_{\mathrm{L}}} + \frac{1-\omega}{T_{\mathrm{E}}},$$

where $\omega = \sigma_{\mathrm{p}}^2/\sigma^2$. From the above relation it follows that $T_{\mathrm{L}}^{*} \to T_{\mathrm{L}}$ at $\tau_{\mathrm{p}} \to 0$ and $T_{\mathrm{L}}^{*} \to T_{\mathrm{E}}$ at $\tau_{\mathrm{p}} \to \infty$.

In [11], the time scale is calculated by the relation

$$T_{\mathrm{L}}^{*} = T_{\mathrm{L}}\left[1 + \frac{\gamma C}{(1 + T_{\mathrm{L}}/\tau_{\mathrm{p}})^{1/2}}\right]^{-1},$$

where $C = (8\pi)^{1/2}$; $\gamma = T_{\mathrm{L}}/T_{\mathrm{E}}$. However, such an approach leads to incorrect limiting relations. In particular, at $\tau_{\mathrm{p}}/T_{\mathrm{L}} >> 1$ (heavy particles) we obtain

$$T_{\mathrm{L}}^{*} = \frac{T_{\mathrm{L}}}{1+\gamma C} = 0.4T_{\mathrm{L}}.$$

Two-step approach. This approach consists of the Lagrange step, where the fluid particle velocity at the time t^{n+1} is calculated from the velocity of the same particle at the time t^{n}, and the following Euler step. At the Euler step the fluid particle velocity at the point where the condensed particle is situated (see Fig. 1) is generated from the velocity at the time t^{n+1} of the fluid particle situated at distance r from the solid particle (this velocity is calculated at the Lagrange step).

The Lagrange (time) step is described by the relation

$$\mathbf{v}_{\mathrm{L}}^{n+1} = a_{\mathrm{L}}\mathbf{v}_{\mathrm{L}}^{n} + b_{\mathrm{L}}\boldsymbol{\xi}_{\mathrm{L}}^{n}. \tag{6}$$

At the Euler (spatial) step the time variables are substituted into their spatial equivalents [24]:

$$\mathbf{v}_{\mathrm{E}}^{n+1} = a_{\mathrm{E}}\mathbf{v}_{\mathrm{L}}^{n+1} + b_{\mathrm{E}}\boldsymbol{\xi}_{\mathrm{E}}^{n+1}. \tag{7}$$

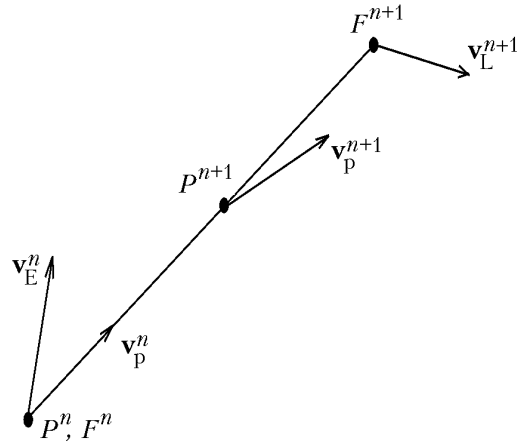

Fig. 2. Position of the condensed particle relative to the fluid particle at the instants of time t^n and t^{n+1}.

Here $\xi_{\mathrm{L}}^n \cup N(0, 1)$; $\xi_{\mathrm{L}}^{n+1} \cup N(0, 1)$. The coefficients a_{L} and b_{L} depend on the form of the Lagrange correlation function, and the coefficients a_{E} and b_{E} are determined by the form of the Euler correlation function.

The distance between the fluid and the solid particles at the time t^{n+1} is expressed in terms of their instantaneous velocities $r = |\mathbf{v}^{n+1} - \mathbf{v}_{\mathrm{p}}^{n+1}|\Delta t$, where $\Delta t = t^{n+1} - t^n$. Because of the spatial correlation anisotropy, the calculated relations are written in the local coordinate system whose x-axis is directed from the fluid particle to the solid one.

For the Lagrange step at $\Delta t \to 0$, Eq. (6) goes over into the Langevin-type equation (3), which has heuristic bases [11]. For the Euler (spatial) step, from (7) we obtain

$$d\mathbf{v} = -\frac{\mathbf{v}}{L_{\mathrm{E}}}\,dx + \sigma\left(\frac{2}{T_{\mathrm{E}}}\right)^{1/2} d\mathbf{w}\,. \tag{8}$$

The velocity difference at the distance r is $\Delta\mathbf{v} = \mathbf{v}(x + r) - \mathbf{v}(x)$. Taking into account that the velocity fluctuations obey the normal probability distribution, we obtain

$$\langle \Delta\mathbf{v} \rangle = 0\,, \quad \left\langle (\Delta\mathbf{v})^2 \right\rangle = 2\sigma^2 \frac{r}{L_{\mathrm{E}}}\,, \quad \left\langle (\Delta\mathbf{v})^3 \right\rangle = 0\,.$$

On the other hand, the Kolmogorov theory gives the following relations [20]:

$$\langle \Delta\mathbf{v} \rangle = 0\,, \quad \left\langle (\Delta\mathbf{v})^2 \right\rangle = (\varepsilon r)^{2/3}\,, \quad \left\langle (\Delta\mathbf{v})^3 \right\rangle = \varepsilon r\,.$$

Consequently, Eq. (8) contradicts the Kolmogorov law in the inertial range. Moreover, Eq. (8) does not admit energy transfer from large vortices to small ones. Unlike Eq. (6) used at the Lagrange step, Eq. (7), which describes the Euler step, has a less sound theoretical basis.

In the model of [22], a finite correlation length $\Lambda \sim L_{\mathrm{E}}$ was introduced. The position of the fluid and solid particles is tracked until the distance between them becomes equal Λ, since the velocities of two turbulent vortices at a distance larger than L_{E} are noncorrelated. At $r > \Lambda$ we assume $R_{\mathrm{E}}(r) = 0$. At $r < \Lambda$ the exponential form of the Euler correlation function is used. In [11], it was shown that such an approach is unsatisfactory for small particles.

Modified approach. In the model of [11], a modified representation of the Euler step described by relation (7) was introduced. The distance between the fluid and the solid particles is calculated by their mean relative velocity: $r = |\langle \mathbf{v}^{n+1} \rangle - \langle \mathbf{v}_{\mathrm{p}}^{n+1} \rangle|\Delta t$. The velocities at the Lagrange and Euler steps are determined by the following relations:

$$\mathbf{v}_{\mathrm{L}}^{n+1} = a_{\mathrm{L}}\mathbf{v}^n + b_{\mathrm{L}}\boldsymbol{\xi}_{\mathrm{L}}^n\,, \quad \mathbf{v}_{\mathrm{E}}^{n+1} = a_{\mathrm{E}}\mathbf{v}_{\mathrm{L}}^{n+1} + b_{\mathrm{E}}\boldsymbol{\xi}_{\mathrm{E}}^{n+1}\,.$$

Using the exponential approximation of the Lagrange and Euler correlation coefficients, we obtain

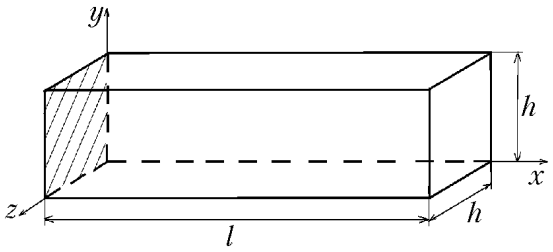

Fig. 3. Coordinate system for the channel flow with injection.

$$a_{\mathrm{L}} = \exp\left(-\frac{\Delta t}{T_{\mathrm{L}}}\right), \quad b_{\mathrm{L}} = \sigma\left(1 - a_{\mathrm{L}}^2\right)^{1/2}, \quad \xi_{\mathrm{L}}^n \in N(0, 1);$$

$$a_{\mathrm{E}} = \exp\left(-\frac{r}{L_{\mathrm{E}}}\right), \quad b_{\mathrm{E}} = \sigma\left(1 - a_{\mathrm{E}}^2\right)^{1/2}, \quad \xi_{\mathrm{E}}^{n+1} \in N(0, 1).$$

The fluid velocity at the point where the solid particle resides at the instant of time t^{n+1} is calculated as

$$\mathbf{v}^{n+1} = a_1 \mathbf{v}_{\mathrm{L}}^{n+1} + a_2 \mathbf{v}_{\mathrm{E}}^{n+1} + b\boldsymbol{\xi}^n. \tag{9}$$

The coefficients a_1, a_2, and b in Eq. (9) depend on the ratio $\sigma_{\mathrm{p}}/\sigma$ and the form of the time correlation function. For large particles, the point P^{n+1} is closer to the point F^n, and for small particles it is closer to F^{n+1}. Particles of medium sizes are positioned between the points F^n and F^{n+1} (Fig. 2).

Unlike the models of [16–18], where $\Delta t \sim 0.2T_{\mathrm{L}}$, the time integration step is chosen from the condition $\Delta t = \min\left\{\Delta t_1, \Delta t_2, \Delta t_3\right\}$, where Δt_1 is the time required for the particle to cross the control volume of the Euler net; $\Delta t_2 = T_{\mathrm{L}}$; $\Delta t_3 = \tau_{\mathrm{p}}$; $\alpha \sim 0.5$.

Results of the Calculations. Let us align the x-axis of the rectangular Cartesian coordinate system with the lower wall of the channel, and the y- and z-axes with its cross-section (Fig. 3). From the upper wall of the channel blowing with velocity v_{w} is carried out. The lower wall is assumed to be impermeable. The channel width and length are chosen to be equal to $h = 0.01$ and $l = 0.30$ m. As a working medium, air is taken.

To calculate the flow, the large eddy simulation method [25] is used. The equations characterizing the flow are written in terms of the space-filtered quantities and coincide formally with nonstationary Reynolds equations. As a model of the subnet eddy viscosity, the Smagorinskii model is used. To obtain molecular viscosity values depending on the temperature, the Sutherland law is used. The filter width is related to the size of the computational mesh width.

At the initial instant of time the velocity component distributions that take place in the vortex flow of a nonviscous liquid are given [26]. The velocity component in the direction of the z-axis is assumed to be equal to zero. On the upper wall, boundary conditions of normal blow with velocity v_{w}, and on the lower wall adhesion and nonpercolation conditions, are formed. The left end wall of the channel is assumed to be impermeable. At the boundary through which the gas leaves the calculated region nonreflective conditions are set. In the direction of the z-axis, periodic boundary conditions (flow repetition conditions) are specified. The blow velocity varies with time by the Gauss law but remains constant in the space. Particles are injected into the channel from the upper wall along the normal to the surface with a velocity equal to the blow velocity.

Discretization of the equations is carried out with the use of the control volume method on a nonuniform mesh and finite-difference schemes with a high time and space resolution [27].

Calculations were performed on a $200 \times 100 \times 50$ mesh with nodes crowding together towards the front bottom (along the x-coordinate) and the impermeable wall (along the y-coordinate) of the channel according to the geometrical progression law. The mesh width on the z-coordinate was assumed to be constant. The time step was $\Delta t = 1.2 \cdot 10^{-5}$ sec. To obtain a statistically stationary flow pattern, 50,000 time steps were made.

To describe the impurity motion and scattering on the basis of the statistical model, it is necessary to calculate the trajectories of a large number of particles. To solve the Cauchy problem, we used methods that made it pos-

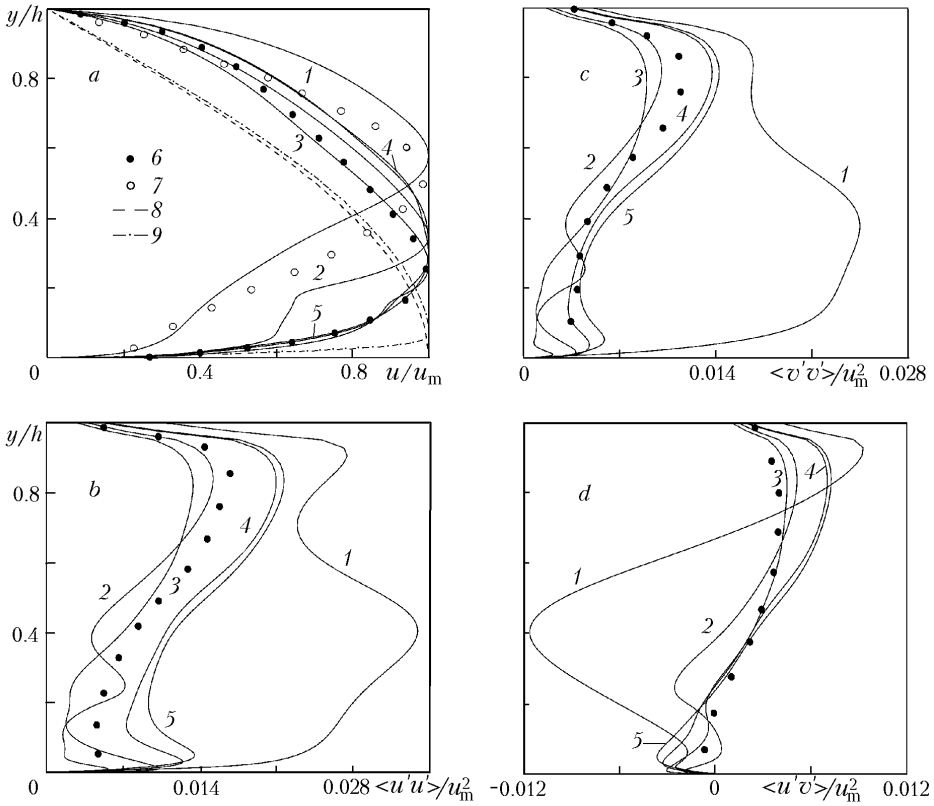

Fig. 4. Distributions of the longitudinal velocity component (a), normal Reynolds stresses $\langle u'u' \rangle$ (b) and $\langle v'v' \rangle$ (c), and shear Reynolds stresses $\langle u'v' \rangle$ (d) over the channel cross-section at $x/h = 30$.

sible to resolve in the solution the fast and slowly decaying components [28]. To supply the carrier gas parameters at the points lying on the particle trajectory, the bilinear interpolation method was used. The integration step along each trajectory was limited by the time and space scales of turbulence. In the calculations, from 1000 to 10,000 trajectories of probe particles depending on their size were modeled.

The distributions of the longitudinal velocity component over the channel cross-section are given in Fig. 4a. The velocity distributions correspond to different velocities of injection from the upper wall of the channel: $v_w = 0.1$ (1); 0.55 (2); 1 (3); 2.75 (4), and 5 m/sec (5). Curve 6 presents the data of the physical experiment of [29]; curve 7 presents the results of the calculation by the k–ε turbulence model at $v_w = 1$ m/sec (conditions for curve (3); curve 8 corresponds to the cosine longitudinal velocity profile taking place in a vortex flow of a nonviscous incompressible liquid; curve 9 shows the velocity profile of a laminar flow of a viscous incompressible liquid at $\mathrm{Re} = 10^3$ [26]. As the Reynolds number increases, the maximum of the longitudinal velocity component approaches the impermeable surface, near which a viscous flow zone similar to the boundary layer on a flat plate develops.

A specific feature of the flow in a channel with injection is the presence of a negative pressure gradient, which strongly influences the mechanism and intensity of turbulent transfer. The calculated distributions of the Reynolds stress tensor components in the channel cross-section are shown in Fig. 4b–d. An increase in the level of turbulent velocity fluctuations is observed in the region of a strong shear at a distance from the permeable wall of the channel where the fluid particles moving normally to the surface have to turn around in the narrow near-surface zone. The results of the calculations are in fair agreement with the data of the physical experiment of [29], excepting the wall-adjacent zones of the flow where the calculation gives a higher turbulence intensity [30].

The results of calculation of the motion and scattering of aluminum oxide particles ($r_p = 5$–10 μm) for various particle sizes (Stokes numbers) are shown in Fig. 5. At the initial instant of time the particle was on the upper wall of the channel. The calculations were made beginning from the point $x_{p0} = 3$ with a step $\Delta x = 0$. The calculation

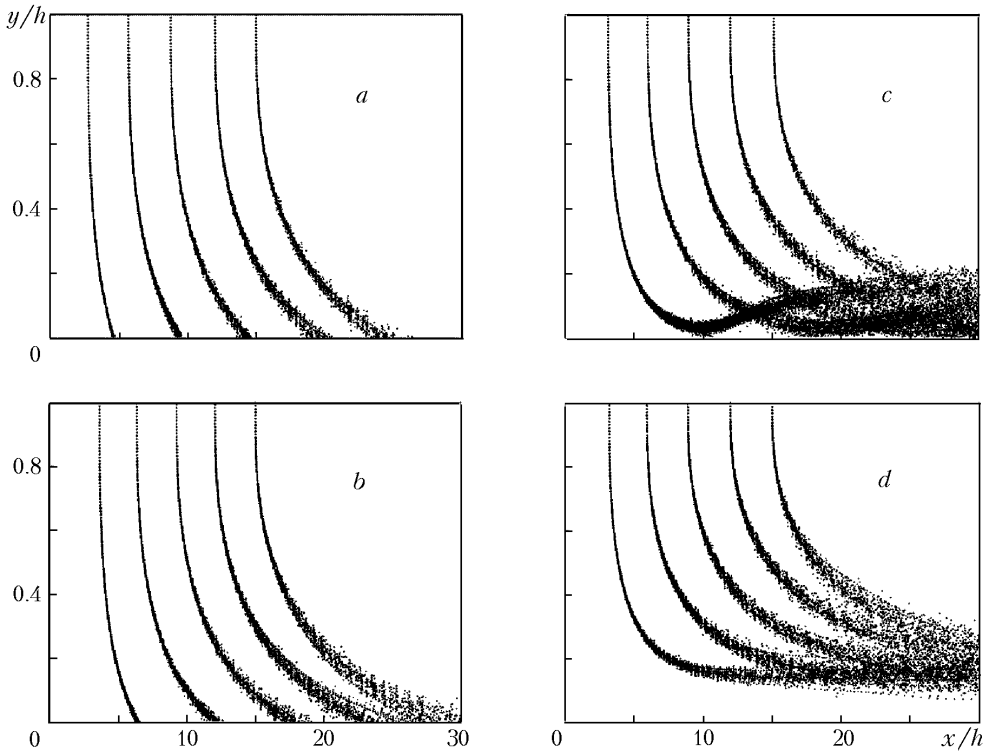

Fig. 5. Particle trajectories in the channel at Stk = 1.0 (a), 0.75 (b), 0.5 (c), 0.25 (d).

was finished when the particle either left the calculated region (at $x/h > 30$) or fell onto the lower wall of the channel (at $y = 0$).

The degree of involvement of a particle in pulsation motion is determined by the relation between the dynamic relaxation time of the particle and the characteristic time scale of turbulence. The inhomogeneity of the carrier phase turbulence field for particles of small fractions leads to the appearance of turbulent migration of the particle (turbophoretic force) in the direction of decreasing pulsation energies of the gas.

For particles of large fractions (r_p = 30–50 μm), velocity fluctuations produce no significant effect on the impurity motion throughout the region of flow development because of the inertia of such particles (Fig. 5a, b). Weak migration of particles towards decreasing pulsation energies of the gas is observed only for particles injected into the channel at a considerable distance from its left end (at $x_{p0} > 9$). Small particles ($r_p \sim$ 5–15 μm) are scattered rather strongly (Fig. 5c, d). The degree of scattering (dispersion of particle displacement) is the higher the smaller the particle size and the farther from the left boundary of the calculated region it is injected into the channel (the kinetic turbulence energy and the rms velocity of the carrier flow vary along the x-coordinate according to a law close to the parabolic one).

The results of the calculations make it possible to determine the time correlation function (correlation coefficient) of a condensed particle along its trajectory. In particular, the definition of the correlation function is given by the relation

$$R_{xx}(t) = \frac{\langle u_p(0)\, u_p(t)\rangle}{\langle u_p^2(0)\rangle^{1/2}\, \langle u_p^2(t)\rangle^{1/2}}.$$

Averaging over the ensemble of random realizations at the instant of time $t = t_0 + i\Delta t$, we obtain

$$R(t_0 + i\Delta t) = \frac{1}{N_p} \sum_i \frac{u_p(t_0)\, u_p(t_0 + i\Delta t)}{\langle u_p^2(t_0)\rangle^{1/2}\, \langle u_p^2(t_0 + i\Delta t)\rangle^{1/2}}.$$

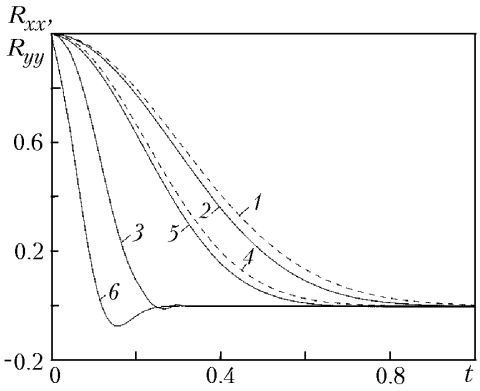

Fig. 6. Longitudinal (1–3) and transverse (4–6) time correlation functions of the carrier flow and the condenser particle at Stk = 0.1 (2, 3) and Stk = 1, 2 (5, 6); curves 1 and 4 correspond to the carrier flow.

The behavior of the longitudinal and transverse correlation coefficients of the particle is shown in Fig. 6 for particles of different sizes (compared to the distribution calculated for the carrier flow).

The correlation function of small particles practically follows the distribution obtained for the carrier flow (small particles are involved in the pulsation motion of the carrier flow and move along the streamlines) and are well described by the exponential dependence often postulated in calculations. At the same time the correlation coefficient of large particles differs in quality from the distribution that takes place for the carrier flow (large particles deviate from the streamlines, largely manifesting their inertia). The transverse correlation coefficient therewith acquires small negative values.

Conclusions. The features of the formulation and realization of various stochastic models of motion and scattering of condensed impurity particles in a turbulent flow have been considered. The possibilities of the stochastic approach based on the integration of a Langevin-type equation have been demonstrated with the example of the calculation of the turbulent flow of a gas suspension in a channel with injection for various values of the injection rate and the sizes of particles and conditions of their introduction into the channel. The results obtained on its basis show that velocity fluctuations of the carrier turbulent flow strongly influence the motion and scattering of dispersive impurity, and the proposed model leads to satisfactory results that agree with the data of numerical and physical experiments.

The application of the method of simulation of large vortices for describing the velocity field of the carrier turbulent flow makes it possible to upgrade the universality of the method, as well as to avoid the application of semiempirical relations for calculating the statistical characteristics of turbulence and the assumption of local inhomogeneity and isotropy of the turbulence field.

NOTATION

a, *b*, coefficients in a discrete Langevin equation; *C*, coefficient; *D*, diffusion coefficient, m^2/sec; *E*, spectral density of the kinetic turbulence energy; *f*, *g*, functions; *G*, convolution kernel; *i*, complex unit; *k*, kinetic energy of turbulence, m^2/sec^2; *l*, channel length, m; *L*, linear scale, m; *N*(0, 1), standard normal probability distribution law; N_p, number of particles; *q*, constant; *r*, radius, m; **r**, radius vector, m; *R*, correlation coefficient; Re, Reynolds number; *t*, time, sec; *T*, time scale, sec; *u*, *v*, velocity components, m/sec; **v**, velocity vector, m/sec; **w**, Wiener random process; *x*, *y*, *z*, spatial coordinates, m; α, β, γ, coefficients; δ, delta function; ε, turbulent energy dissipation rate, m^2/sec^3; κ, wave number, 1/m; Λ, correlation length, m; μ, dynamic viscosity, kg/(m·sec); ξ, vector of random numbers that are chosen from the normal probability distribution with zero mathematical expectation and unit dispersion; ρ, density, kg/m^3; σ, rms value of velocity fluctuation, m/sec; τ, relaxation time, sec; φ, basics element; ω, velocity dispersion ratio between the particle and the carrier flow. Subscripts: d, particle drag; E, Euler characteristics of turbulence; *i*, *j*, summation indices; K, characteristics of turbulence in the inertial interval obeying the Kolmogorov law; L, Lagrange

characteristics of turbulence; m, maximum; p, particle; t, turbulent; w, wall; 0, initial instant of time; ′, fluctuations of parameters; ∗, convolution.

REFERENCES

1. K. N. Volkov, Stochastic modeling of impurity motion and scattering in the mechanics of turbulent gas-dispersed flows, *Inzh.-Fiz. Zh.*, **77**, No. 5, 10–20 (2005).
2. É. P. Volkov, L. I. Zaichik, and V. A. Pershukov, *Modeling of Solid Fuel Combustion* [in Russian], Nauka, Moscow (1994).
3. A. A. Shraiber, L. B. Gavin, V. A. Naumov, and V. P. Yatsenko, *Turbulent Gas Suspension Flows* [in Russian], Naukova Dumka, Kiev (1987).
4. C. T. Crowe, T. R. Troutt, and J. N. Chung, Numerical models for two-phase turbulent flows, *Ann. Rev. Fluid Mech.*, **28**, 11–43 (1996).
5. A. D. Gosman and E. Ioannides, Aspects of computer simulation of liquid-fueled combustors, *AIAA Paper*, No. 81-0323 (1981).
6. M. Sommerfeld and G. Zivkovic, Recent advances in the numerical simulation of pneumatic conveying through systems, in: *Computational Methods in Applied Sciences*, Elsevier Science Ltd, Amsterdam (1992), pp. 201–212.
7. D. Lakehal, On the modelling of multiphase turbulent flows for environmental and hydrodynamic applications, *Int. J. Multiphase Flow*, **28**, No. 5, 823–863 (2002).
8. S. B. Pope, Lagrangian modeling of turbulent flows, *Ann. Rev. Fluid Mech.*, **26**, 23–63 (1994).
9. Y. Mito and T. J. Hanratty, Lagrangian stochastic simulation of turbulent dispersion of heat markers in a channel flow, *Int. J. Heat Mass Transfer*, **46**, No. 6, 1063–1073 (2003).
10. R. Rzehak and W. Zimmermann, Inertial effects in Brownian motion of a trapped particle in shear flow, *Physica A*, **324**, 495–508 (2003).
11. J. Pozorski and J.-P. Minier, On the Lagrangian turbulent dispersion models based on the Langevin equation, *Int. J. Multiphase Flow*, **24**, No. 6, 913–945 (1998).
12. K. N. Volkov, Influence of turbulence on the deposition of particles from a gas-dispersed flow onto the wall, *Inzh.-Fiz. Zh.*, **77**, No. 5, 20–29 (2005).
13. J.-P. Minier and E. Peirano, The PDF approach to turbulent polydispersed two-phase flows, *Physics Report*, **352**, 1–214 (2001).
14. A. M. Reynolds, A Lagrangian stochastic model for particle trajectories in non-Gaussian turbulent flows, *Fluid Dyn. Res.*, **19**, 277–288 (1997).
15. S. B. Pope, PDE methods for turbulent reactive flows, *Progr. Energy Combust. Sci.*, **11**, 119–192 (1985).
16. M. Sommerfeld, Validation of a stochastic Lagrangian modeling approach for interparticle collisions in homogeneous isotropic turbulence, *Int. J. Multiphase Flow*, **27**, No. 11, 1829–1858 (2001).
17. D. Huilier, On the necessity of including the turbulence experienced by an inertial particle in Lagrangian random-walk models, *Mech. Res. Commun.*, **31**, 237–242 (2004).
18. J. Lataste, D. Huilier, and H. Burnage, Influence of the fluid turbulence on the dispersion of heavy particles in a turbulent boundary layer, *Acad. of Sci. Paris*, **327**, No. 8, 731–738 (1999).
19. P. A. Durbin, A random flight model of inhomogeneous turbulent dispersion, *Phys. Fluid*, **31**, 2151–2153 (1980).
20. J. O. Hinze, *Turbulence*, McGraw-Hill, New York (1975).
21. G. T. Csanady, Turbulent diffusion of heavy particles in the atmosphere, *J. Atmos. Sci.*, **20**, 201–208 (1963).
22. A. Berlemont, Desjonqueres, and G. Gouesbet, Particle Lagrangian simulation in turbulent flows, *Int. J. Multiphase Flow*, **16**, No. 1, 19–34 (1990).
23. D. Burry and G. Bergeles, Dispersion of particles in anisotropic turbulent flows, *Int. J. Multiphase Flow*, **19**, No. 4, 651–664 (1993).
24. Q. Zhou and M. A. Leschziner, A Lagrangian particle dispersion model based on a time-correlated stochastic approach, *Gas-Solid Flows*, **121**, 255–260 (1991).

25. K. N. Volkov, Large-eddy simulation of turbulent gas-particle flows in the duct induced by the wall injection, in: *Computational Fluid and Solid Mechanics*, Elsevier Science Ltd, Amsterdam (2005), pp. 928–931.
26. K. N. Volkov and V. N. Emel'yanov, Mathematical models of three-dimensional turbulent flows in channels with injection, *Mat. Modelir.*, **16**, No. 10, 41–63 (2004).
27. K. N. Volkov, Application of the control volume method for solving the problems of fluid mechanics on non-structured grids, *Vychisl. Metody Programmir.*, **6**, No. 1, 43–60 (2005).
28. K. N. Volkov, Difference schemes of integration of the equations of probe particle motion in a liquid or a gas flow, *Vychisl. Metody Programmir.*, **5**, No. 1, 5–21 (2004).
29. B. Chaouat, Numerical simulation of channel flows with fluid injection using Reynolds stress model, *AIAA Paper*, No. 2000-0992 (2000).
30. A. Kourta, Instability of channel flow with fluid injection and partial vortex shedding, *Comput. Fluids*, **33**, 155–178 (2004).